ARTICLE

Counting Radio-Krypton Atoms with a Laser†

Guo-min Yang[a], Le-yi Tu[a], Cun-feng Cheng[a], Xiang-yang Zhang[a,b], Shui-ming Hu[a]*

a. Hefei National Laboratory for Physical Sciences at the Microscale, University of Science and Technology of China, Hefei 230026, China
b. Institute of Hydrogeology and Environmental Geology, Chinese Academy of Geological Sciences, Shijiazhuang 050061, China

(Dated: Received on May 26, 2015; Accepted on July 26, 2015)

Because of their unique chemical and physical properties, long-lived rare krypton radioisotopes, ^{85}Kr and ^{81}Kr, are ideal tracers for environmental samples, including air, groundwater and ice. Atom trap trace analysis (ATTA) is a new laser-based method for counting both ^{85}Kr and ^{81}Kr atoms with the abundance as low as 10^{-14} with micro-liters (STP) krypton gas. The entire system for rare radio-krypton measurement built at Hefei is presented, including the atom trap trace analysis instrument and sampling apparatus of gas extraction from water and krypton purification. Atmospheric ^{85}Kr concentrations at different places in China were measured, showing a range of 1.3−1.6 Bq/m^3, consistent with the northern hemispheric baseline. As a demonstration of the system, some shallow and deep groundwater samples in north and south China were sampled and dated.

Key words: Atom trap trace analysis, ^{85}Kr, ^{81}Kr, Groundwater, Dating

I. INTRODUCTION

^{85}Kr and ^{81}Kr are two long-lived rare radioisotopes of the krypton element. Krypton gas mainly resides in the atmosphere, at concentration of 1.14 ppm [1]. Because of its unique chemical inertness, short gas-water dissolution equilibrium time, and well recorded atmospheric contents, krypton gas has relative simple mechanisms during the transport and mixing processes, and radio-krypton has wide applications in the research of paleoclimatology and geohydrology.

^{85}Kr ($t_{1/2}$=10.7 year [2]) is a fission product, mainly released by human nuclear activities during the nuclear era. The atmospheric concentration of ^{85}Kr has been increased by 6 orders of magnitude up to 1.5 Bq/m^3 during the past 70 years [3], corresponding to ^{85}Kr/Kr=2.5×10^{-11} nowadays. The transport time from the northern to the southern hemisphere was estimated to be 1.1 years [4]. Since main sources, as nuclear reprocessing plants, are located in the northern hemisphere [3], the ^{85}Kr baseline there is about 15% higher than that in the southern hemisphere [5]. With well recorded atmospheric contents, ^{85}Kr is an ideal tracer to construct and test the global atmospheric transport model [6], and a sensitive indicator of clandestine plutonium separation [7, 8] and nuclear reactor safety [9]. ^{85}Kr has wide applications in dating shallow groundwater in the age of range 2−50 years without the problems as degradation and decline [10, 11].

^{81}Kr ($t_{1/2}$=229,000 year [12]) is mainly produced through the cosmic ray-induced spallation of stable krypton isotopes in the atmosphere [13]. The atmospheric ^{81}Kr/Kr abundance is about $(5.3\pm1.2)\times10^{-13}$ [14], with a uniform spatial distribution and temporally constant. The fission process, especially the β^- decay chain, is stopped by the stable isotope ^{81}Br on the neutron-rich side of ^{81}Kr. Anthropogenic and subsurface production of ^{81}Kr is negligible. Compared to ^{36}Cl ($t_{1/2}$=301000 year) dating [15, 16], ^{81}Kr is an ideal tracer for dating groundwater and ices in the age range of 5×10^5 to 1×10^6, without complex sources and mixing process.

Several methods have been developed to detect the above rare radioisotopes. Low-level counting (LLC) [17, 18] and liquid scintillation counting (LSC) [19] can routinely analyze ^{85}Kr by counting emitted β^--decay rays, with a typical krypton volume of 20 and 700 μL respectively. Due to the long lifetime of ^{81}Kr and the unavoidable large background of ^{85}Kr, it is impractical to count ^{81}Kr by LLC or by LSC. Accelerator mass spectroscopy (AMS) [14, 20] has been used to date ^{81}Kr using 500 μL of krypton extracted from 16 tons of groundwater. The low efficiency and isobar interference make it difficult for ^{81}Kr dating. Resonance ionization mass spectrometry (RIMS) [21, 22] was applied to measuring the ^{81}Kr in the Milk River aquifer, Canada. With the problems of poor isotope selectivity and pre-enrichment unsolved, RIMS has so far not worked successfully at multisamples. Atom trap trace analysis (ATTA) [23] is

†Dedicated to Professor Qing-shi Zhu on the occasion of his 70th birthday.
*Author to whom correspondence should be addressed. E-mail: smhu@ustc.edu.cn

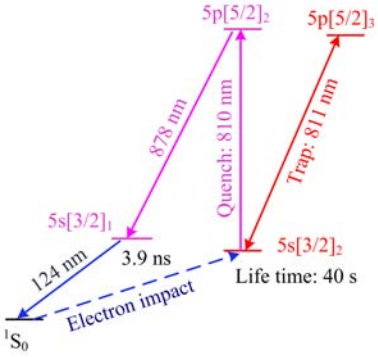

FIG. 1 Energy levels and transitions related to the ATTA measurement of Kr.

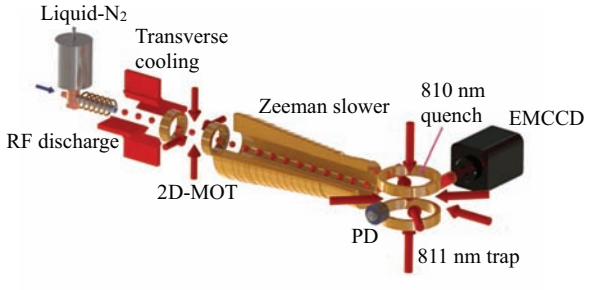

FIG. 2 Schematic of the ATTA instrument.

a laser-based method, counting particular rare isotope atoms in a magneto-optic trap (MOT) with micro-liters (STP) of sample gas [24, 25]. Only atoms resonating with the laser frequency will be trapped and detected, without interference from any other species. Relative abundances of ^{85}Kr/Kr and ^{81}Kr/Kr can be determined together in one measurement tuning laser frequency.

In this work, the apparatus of radio-krypton measurement built at Hefei is introduced. First, the structure of the ATTA setup is presented. A sampling system is described, including gas extraction and krypton purification. Krypton gas of micro-liters is separated from air samples or dissolved gas extracted from groundwater samples. Finally, as a demonstration, measurements of some environmental samples are shown, including determining the ^{85}Kr concentration in the atmosphere and ^{81}Kr/^{85}Kr dating of groundwater.

II. EXPERIMENTAL SETUP

A. The ATTA-USTC apparatus

A diagram of the energy levels of krypton is presented in Fig.1. Due to the 124 nm $^1S_0 \rightarrow 5s[3/2]_1$ electric dipole transition lying in VUV region, there is no laser available for cooling and trapping krypton atoms from the ground state. Thanks to the metastable state ($5s[3/2]_2$, life time 40 s), there exists a $5s[3/2]_2 \rightarrow 5p[5/2]_3$ cycling transition suitable for manipulation using mature near-infrared lasers.

A schematic of the ATTA instrument is shown in Fig.2. Metastable krypton atoms (Kr*) are first produced by an RF-driven discharge inside a liquid-N_2 cooled AlN ceramic tube. Divergences of the Kr* atomic beam is transversely compressed by 811 nm resonating laser beams reflected between mirrors [26]. A 2D-MOT is applied to slightly focus the collimated atomic beam. The high intensity atomic beam is slowed in a Zeeman slower. Kr* atoms are then trapped in the MOT. The number of trapped Kr* atoms, N, can be described by a simple equation:

$$\frac{\mathrm{d}N}{\mathrm{d}t} = L - \alpha N - \beta N^2 \tag{1}$$

where L is the loading rate of the MOT, α is the collision loss rate with background gas, and β is the collision loss rate between trapped atoms. More than 10^8 ^{83}Kr (^{83}Kr/Kr=11.5%) atoms accumulate in the MOT, with a loading rate $\sim 10^{10}$ s^{-1}. For the rare radioisotopes, ^{85}Kr and ^{81}Kr, whose abundances are 10 orders of magnitude lower than that of ^{83}Kr, only individual atoms are trapped at a time, with a life time of a few hundred milliseconds in the trap. The photons emitted from trapped atoms are imaged by a sensitive EMCCD camera. Signal of a single trapped atom can be distinguished from the background of scattering light, with a signal-to-noise ratio of 15. We set 5 standard deviations above background as the atom identification threshold and obtain the isotopic abundance from the atom counting rate, which in principle are proportional to each other.

Due to fluctuations in the experimental conditions, such as pressure, laser intensity and frequency, the counting efficiency may drift slowly. A "quench and capture" method is used to determine the loading rate of the stable isotope ^{83}Kr, as a reference to normalize the counting efficiency [27]. Trap is turned on and off on the order of microseconds by a 810 nm laser beam, frequency stabilized on resonance with the $5s[3/2]_2 \rightarrow 5p[5/2]_2$ transition. During the first few milliseconds of the loading process, the third term on right side of Eq.(1) is negligible, yielding

$$N = \frac{L}{\alpha}(1 - \mathrm{e}^{-\alpha t}) \tag{2}$$

Fluorescence from the atom cloud is detected by a photodiode. The ^{83}Kr loading rate is obtained by fitting the signals via Eq.(2). During the measurement, the trap laser frequency is switched between ^{83}Kr and the rare radioisotopes every few minutes. Four commercial krypton sample gases bought in different years were tested, referred as sample a−d. Samples a and c were known as produced in 2012 and 2007 respectively, and were measured in June 2012. Samples b and d have unknown production years and were measured in March

DOI:10.1063/1674-0068/28/cjcp1505108

2013. Over at least two orders of the dynamic range, the ratio of the rare radioisotopes to ^{83}Kr of the same sample shows excellent proportionality, as illustrated in Fig.3. The difference between a and c agrees reasonably with the half-life time of ^{85}Kr, and the production years of samples b and d can be estimated to be 2010 and 2002, respectively. The measured ^{81}Kr counting rates of the modern krypton gas sample are also shown in Fig.3.

The quantitative reliability and capability of ATTA have been verified by a comparison with different instruments [25]. A group of 12 samples with ^{85}Kr/Kr ratios in the range of 10^{-13} to 10^{-10} were measured independently in three laboratories, the LLC laboratory in Bern (Switzerland), and two ATTA laboratories at Hefei (China) and Argonne (USA). The results show excellent agreement at 5% level.

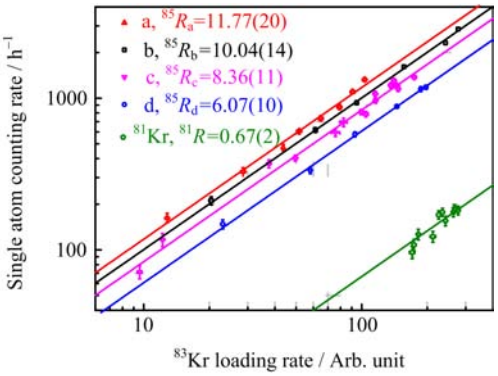

FIG. 3 Ratio between the ^{85}Kr counting rate and the ^{83}Kr loading rate measured by the ATTA-Hefei setup. Four commercial krypton gas samples were used, referred as samples a, b, c, and d. Samples a and c were produced in 2012 and 2007 respectively.

B. Uncertainty in ATTA measurement

Using a RF discharge puts some limitations on the measurement. The minimum pressure required to maintain a stable discharge limits the sample size. This can be overcome with mixing pure xenon gas with the sample. Krypton atoms will also be ionized and accelerated during their excitation into metastable states. Some of the krypton atoms with high kinetic energy will be implanted into the inner walls of the vacuum chamber, while krypton atoms implanted during previous measurements will be released back into the system, causing a cross-sample contamination. A 36 h flushing of pure xenon gas discharge following each measurement is implemented to reduce such memory effect and bring outgassing rates down to an acceptable level of 0.02 μL per hour. Such a solution limits the measurement process to a two-day period, even though only 4 h of counting is carried out. The memory effect also restricts the sample size and counting time.

The uncertainty in derived rare isotope abundances includes those from the ^{83}Kr measurement, statistics in atom counting, and cross-sample contamination. The uncertainty in ^{83}Kr measurement is about 2%−3%, while others depend on the radioisotopes concentration and the sample size. Since the counting efficiency is proportional to the radioisotopes concentration and approximate sample size, a small or old sample (with depleted radio-krypton) will have larger atom statistics errors and a greater contamination effect. The typical sample size required for counting ^{85}Kr and ^{81}Kr is 5−10 μL, corresponding to approximately 5−10 L air, 100−200 L water, or 40−80 kg ice. Relative isotope abundance in modern samples of such size can be determined at an uncertainty level of 5%−10%. For ^{81}Kr dating applications, ATTA covers an age range from 150000 year to 1500000 year, with a relative 10%−20% error. For ^{85}Kr/Kr analysis, the required sample size can be reduced to 1 μL, because the initial isotope abundance is an order of magnitude higher than that of ^{81}Kr in the atmosphere. The purity of krypton gas is not strictly required, since the relative ratios of krypton isotopes are not affected by other impurity gases.

C. Gas extraction from water samples

Field gas extraction is required as relatively large amounts of water needed to be sampled to satisfy the requirements of dating. According to Henry's law, dissolved gas will be released from water when exposed to a vacuum environment. Some characteristics of such systems must be satisfied: (i) be well sealed to avoid ambient air contamination, (ii) high extraction yield and speed to minimize the water volume and extraction time, (iii) be sufficiently robust and convenient for field work. There are two methods to realize the extraction, vacuum extraction chambers [28] and membrane contactors [29]. We set up an apparatus of the first type and describe it as follows.

The diagram of the vacuum extraction system is shown in Fig.4. A diaphragm pump is first used to prepare the vacuum before field working. Sand in the water pumped from the wells are filtered out by cotton filters. The water pressure is increased by a booster pump to satisfy the atomization. A pressure gauge and a flow meter record the water pressure and flux. Water is sprayed through 4 atomizer nozzles into a transparent cylinder made of plexiglass. At the bottom of the cylinder, water is continuously pumped out by magnetic drive pumps which can work at negative pressure. The water flux is controlled to match the pump rate and to reach a dynamic equilibrium of water levels. Gas at the top of the cylinder is continuously transferred to a pre-vacuumed sample container (typically 4 L) through a compressor.

An extraction yield higher than 75% is reached, ac-

DOI:10.1063/1674-0068/28/cjcp1505108

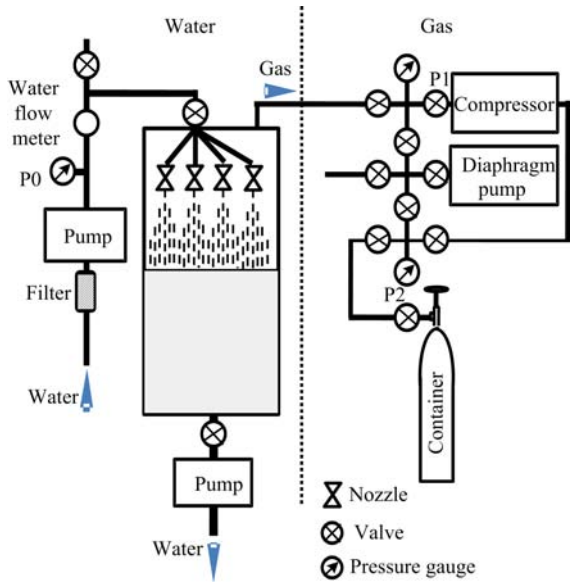

FIG. 4 Diagram of vacuum extraction system built at USTC.

cording to the oxygen concentration before and after extraction measured by a dissolved oxygen meter. The flow rate is about 5−8 L/min, mainly limited by the drainage pump. The leak rate is about 5 Pa·L/min, which represents less than 0.1% contamination from modern air during 2 h operation. The groundwater sampling apparatus has a size of 50 cm (length)×34 cm (width)×60 cm (height) and an overall weight of about 40 kg. A new system is under built to reduce its weight to about 20 kg.

D. Krypton purification

The two steps of the purification process [30], cryogenic distillation and gas chromatography (GC) separation, are applied to separate ppm-level krypton from a large quantity of gas which have been collected from environmental samples. Unlike ambient air, dissolved gas from groundwater may have depleted oxygen but sometimes excess CO_2 or CH_4. The diagram of the krypton purification process is shown in Fig.5 and described below.

After removing CO_2 and H_2O through a molecular sieve 5A, the gas sample is condensed in a liquid-N_2 cooled trap filled with activated charcoal. The flow rate and the total volume of the gas are recorded by a mass flow controller (MFC). A rotary pump slowly pumps out the gases above the trap, with the pumping rate of 0.2 L/min constrained and monitored by the MFC. During the cryogenic distillation process, Kr is enriched in the residual phase, since it has much lower vapor pressure than the major constituents (N_2, O_2 and Ar). When most of the gases have been pumped out, a drop in the pumping rate occurs, as an indicator to end the distillation process. The distillation residue is sent into a furnace (1000 K) containing Ti, where the residual active gases including N_2, O_2, hydrocarbon molecules, especially CH_4, are removed. The sample gas volume is reduced to about 10 mL, then carried by pure helium into the GC operating at room temperature with a 2-m-long molecular sieve 5A chromatographic column. Gas is collected during the Kr peak elution time. Due to overlapping with the N_2 peak tail, a second run of chromatographic separation is needed to increase the purity of obtained krypton gas.

The performance of the purification system is shown in Fig.6. Yield ratios over 90% are realized with an air sample of up to 20 L. Due to a minor leak in the commercial GC apparatus, a constant amount of 0.5 μL of Ar is contained in the purified Kr, corresponding to a negligible Kr leak from ambient air. The purity of Kr decreases from 97% to 73% when reducing the quantity of air from 20 L to 1 L. Since ATTA measures relative ratio between the rare and abundant krypton isotopes, the residual argon has no effect on the results given by ATTA measurements.

III. APPLICATIONS

A. Atmospheric ^{85}Kr concentration

Emissions of nuclear reprocessing plants with well known release time, serving as ^{85}Kr point sources, can be used to test the global atmospheric transport model. A global surface atmospheric ^{85}Kr concentration was obtained through the model and compared with a series of observation sites [6]. The northern hemispheric baseline was about 1.4−1.5 Bq/m^3 between 2006 and 2013 [31], showing a slight decrease of about 30 mBq/m^3 at the first 5 years, then increasing about 30 mBq/m^3 per year. Due to the reprocessing plants located in Russia and Japan continuously releasing ^{85}Kr, a significant latitudinal distribution of atmospheric ^{85}Kr level in China is predicted from the model. ^{85}Kr concentration decreased more than 10% from north to south China in 2006.

Several air samples were collected, located in urban Hefei city, Guangdong, Hebei provinces and the northwest regions of Gansu and Xinjiang provinces, as shown in Fig.7. Most of the samples were only measured once with about 5% uncertainties, comparable with the regional differences. The data of Gansu and Hefei (2013) were an average of two and five measurements, respectively. The ^{85}Kr concentrations vary between 1.3−1.6 Bq/m^3 in the past two years, consistent with the northern hemispheric baseline. The results present a rough latitudinal distribution that matches the model given in Ref.[6]. More frequent sampling is required to outline the temporal and spatial distribution. A time resolution of two days, limited by the memory effect, can be achieved with a full run with one

DOI:10.1063/1674-0068/28/cjcp1505108

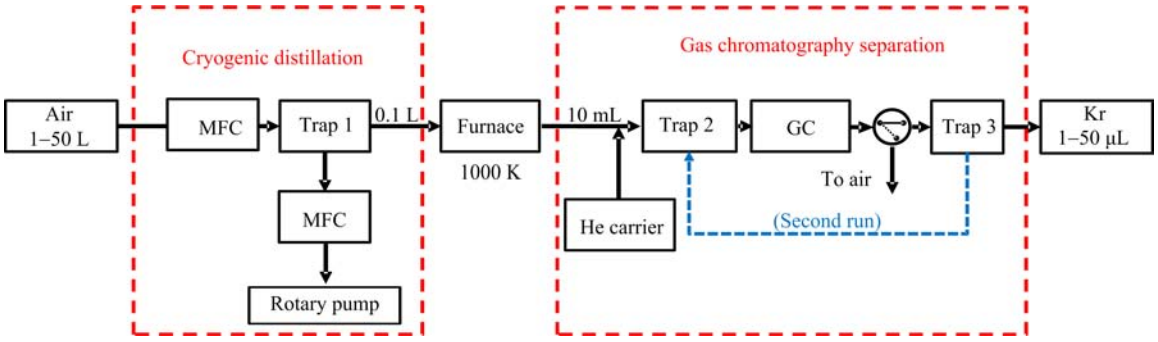

FIG. 5 Diagram of the krypton purification process. MFC: mass flow controller, GC: gas chromatography, trap: liquid-nitrogen cooled trap filled with activated charcoal.

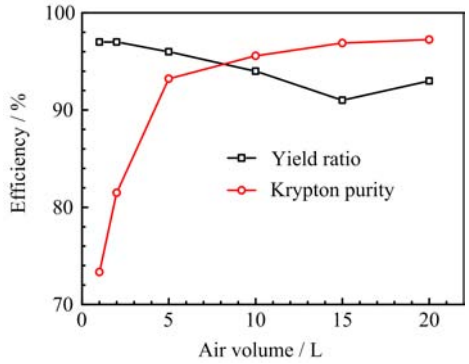

FIG. 6 Performances of the purification system at different ambient air size.

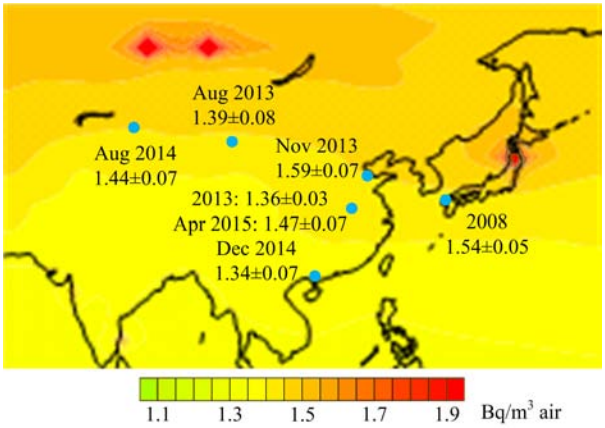

FIG. 7 Atmospheric ^{85}Kr concentration in China. The background is the annual surface ^{85}Kr concentration in 2006 [6]. The compare data in Japan is from Ref.[19].

setup, which will give more information in comparison with the weekly sampling [6].

B. ^{81}Kr and ^{85}Kr dating of groundwater

Four groundwater samples were sampled in the field. Samples No.10057 and No.10061 locates in North China Plain (NCP), samples No.10074 and No.10075 locates at South China (SC). The results are given in Table I. ^{85}Kr is in the unit of Bq/m^3, and ^{81}Kr is in the unit of percent modern krypton (pMKr).

There are two shallow groundwater samples (No.10057, No.10074). All the ^{85}Kr activity is low, about 20%−60% of the atmospheric level, which means their ages are younger than 50 years. ^{81}Kr/Kr ratios in the three samples agree with modern ^{81}Kr levels. In order to get the apparent ^{85}Kr age, an atmosphere input function is required. It is extracted and combined from Refs.[31, 32], as shown in Fig.8. A local air sample was measured as shown above, and is used to correct the northern hemispheric ^{85}Kr baseline curve as local input function. A 10% uncertainty in the input function may be considered appropriately. Here this uncertainty is not considered in determining the ages of the samples, causing an underestimated age error. The apparent ^{85}Kr age can be determined by plotting the ^{85}Kr activity and sampling date and following the decay lines back to the atmosphere input function curve. The ^{85}Kr age of No.10074 sample (SC) is only 6.3 years, indicating a high groundwater renewal ability. The apparent ^{85}Kr age of sample No.10057 are 20.4 years. The results are about 10 years younger than that given by ^{3}H-^{3}He dating [33]. This is probably because of the krypton exchange between groundwater and the air in the soil, since the groundwater level is low due to over exploitation. The determined ^{85}Kr activities of the samples No.10061, No.10075 are less than 1% of the background of the atmosphere, well below the noise level of the ATTA instrument. The very low ^{85}Kr concentrations mean that the ages of these two samples are older than 50 years, also indicating that air contamination during sampling and young groundwater mixing processes are negligible.

During the past million years, the ^{81}Kr abundance has decreased by about 10% due to the paleointensity change in the geomagnetic field [34]. This causes an underestimated age error, less than 4%, based on the stable ^{81}Kr/Kr assumption. Here we do not consider this

DOI:10.1063/1674-0068/28/cjcp1505108

TABLE I Groundwater samples for ^{85}Kr and ^{81}Kr.

Trace No.	Gas/L	Date	^{85}Kr activity[a]/(Bq/m^3)	^{81}Kr/pMKr[b]	^{85}Kr age[c]/year	^{81}Kr age/10^3 year
10074(SC)	6.6	Apr 2 2015	0.84±0.049	99±7	6.3±1.1	Modern
10057(NCP)	5.5	Feb 9 2014	0.312±0.017	108±6	20.4±0.6	Modern
10061(NCP)	11.2	Mar 9 2015	0.008±0.004	106±6	>50	Modern
10075(SC)	7.8	Apr 4 2015	0.004±0.004	45±3	>50	264±22

[a] Value of 1.14 ppm for krypton in air is used.
[b] pMKr: percent modern krypton.
[c] Age: time from recharge area to sampling site. NCP samples were sampled in April 2014, and SC samples were sampled in December 2014.

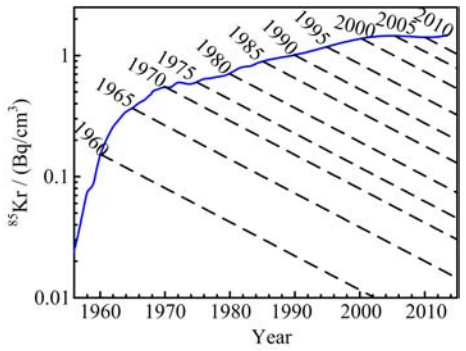

FIG. 8 Northern hemispheric ^{85}Kr activity as a function of time, extracted and combined from Refs.[31, 32]. Dashed diagonal lines represent radioactive decay since isolation from the atmosphere. Note that a logarithmic scale is used.

factor in determining the ^{81}Kr ages of the old groundwater samples (No.10061, No.10075), and simply use a stable input function. Sample No.10061 has a depleted ^{85}Kr concentration, but its ^{81}Kr is close to the modern value, indicating an age elder than 50 years but younger than 50000 years. The ^{81}Kr concentration of sample No.10075 is about half of the modern value. Therefore, the ^{81}Kr age of sample No.10075 is determined to be 264000 years. To the best of our knowledge, this is the first time that such old groundwater is found in this area. The detailed geological analysis will be presented in a separated study.

IV. CONCLUSION

A complete system for measuring ^{85}Kr and ^{81}Kr in environmental samples is presented. Typically 5−10 μL of krypton gas is required to meet the measurement standards by the ATTA instrument, which is based on a magneto-optic trap. Relative isotope abundance of modern samples can be determined at an uncertainty level of 5%−10% by counting individual atoms. The entire measurement process will take two days, limited by the xenon flushing due to the memory effect. A simple and portable water sampling apparatus extracting dissolved gas from groundwater was also built. Gas of 10 L can be extracted from groundwater in 2 h operation in the field, with an efficiency of over 75%. Krypton gas in air-like samples of 1−50 L can be separated using a combined process of cryogenic distillation and gas chromatography, with a yield efficiency of 90%. Some applications have been demonstrated using the system. Atmospheric ^{85}Kr concentrations in the range of 1.3−1.6 Bq/m^3 in China were determined, consistent with the northern hemispheric baseline. Shallow and deep groundwater samples in south and north China were sampled and dated. Groundwater older than 200000 years was found in south China for the first time by ^{81}Kr dating.

Further improvements in ATTA are underway to increase the detection efficiency and to reduce the sample size. If the detection efficiency is improved with an order of magnitude, routine ATTA measurement of another radioactive noble gas isotope, ^{39}Ar ($t_{1/2}$=269 year) with a much lower abundance (^{39}Ar/Ar=8.1×10^{-16}) will be feasible, as demonstrated in a proof-of-principle study [35, 36]. ^{39}Ar dating fills the gap between ^{85}Kr and ^{14}C, and have wide applications including the studies of ocean ventilation [37].

V. ACKNOWLEDGMENTS

This work is supported by the National Natural Science Foundation of China (No.21225314, No.41102151), and Special Fund for Land and Resources Research in the Public Interest (No.201511046). Z. Y. Chen from IHEG-CAGS, and J. Y. Chen from Sun Yat-Sen University are acknowledged for providing the testing groundwater samples. The groundwater sampling in South China was supported by INQUA-IFG1309F, IGCP-618 and Guangdong Bureau of Water Conservation (2014-2016).

[1] F. Verniani, J. Geophys. Res. **71**, 385 (1966).

DOI:10.1063/1674-0068/28/cjcp1505108

[2] B. Singh and J. Chen, Nuclear Data Sheets **116**, 1 (2014).
[3] J. Ahlswede, S. Hebel, J. O. Ross, R. Schoetter, and M. B. Kalinowski, J. Environ. Radioact. **115**, 34 (2013).
[4] D. J. Jacob, M. J. Prather, S. C. Wofsy, and M. B. McElroy, J. Geophys. Res. Atmos. **92**, 6614 (1987).
[5] A. Bollhöfer, C. Schlosser, J. O. Ross, H. Sartorius, and S. Schmid, J. Environ. Radioact. **127**, 111 (2014).
[6] J. O. Ross, *Ph.D. thesis*, University of Hamburg (2010).
[7] M. B. Kalinowski, H. Sartorius, S. Uhl, and W. Weiss, J. Environ. Radioact. **73**, 203 (2004).
[8] R. C. Kemp, J. Environ. Radioact. **99**, 1341 (2008).
[9] W. Nitta, T. Sanada, K. Isogai, and C. Schlosser, J. Nuclear Sci. Technol. **51**, 712 (2014).
[10] B. Ekwurzel, P. Schlosser, W. M. Smethie, L. N. Plummer, E. Busenberg, R. L. Michel, R. Weppernig, and M. Stute, Wat. Resour. Res. **30**, 1693 (1994).
[11] M. Kralik, F. Humer, J. Fank, T. Harum, G. Klammler, D. Gooddy, J. Sültenfuss, C. Gerber, and R. Purtschert, Appl. Geochem. **50**, 150 (2014).
[12] C. M. Baglin, Nuclear Data Sheets **109**, 2257 (2008).
[13] W. Kutschera, M. Paul, I. Ahmad, T. A. Antaya, P. J. Billquist, B. G. Glagola, R. Harkewicz, M. Hellstrom, D. J. Morrissey, R. C. Pardo, K. E. Rehm, B. M. Sherrill, and M. Steiner, Nucl. Instrum. Meth. B **92**, 241 (1994).
[14] P. Collon, T. Antaya, B. Davids, M. Fauerbach, R. Harkewicz, M. Hellstrom, W. Kutschera, D. Morrissey, R. Pardo, M. Paul, B. Sherrill, and M. Steiner, Nucl. Instrum. Meth. B **123**, 122 (1997).
[15] J. Park, C. M. Bethke, T. Torgersen, and T. M. Johnson, Wat. Resour. Res. **38**, 1043 (2002).
[16] B. E. Lehmann, A. Love, R. Purtschert, P. Collon, H. H. Loosli, W. Kutschera, U. Beyerle, W. Aeschbach-Hertig, R. Kipfer, S. K. Frape, A. Herczeg, J. Moran, I. N. Tolstikhin, and M. Gröning, Ear. Planet. Sci. Lett. **211**, 237 (2003).
[17] H. H. Loosli, M. Heimann, and H. Oeschger, Radiocarbon **22**, 461 (1980).
[18] H. H. Loosli, M. Mőll, H. Oeschger, and U. Schotterer, Nuc. Instrum. Meth. B **17**, 402 (1986).
[19] N. Momoshima, F. Inoue, S. Sugihara, J. Shimada, and M. Taniguchi, J. Environ. Radioact. **101**, 615 (2010).
[20] P. Collon, W. Kutschera, H. H. Loosli, B. E. Lehmann, R. Purtschert, A. Love, L. Sampson, D. Anthony, D. Cole, B. Davids, D. J. Morrissey, B. M. Sherrill, M. Steiner, R. C. Pardo, and M. Paul, Ear. Planet. Sci. Lett. **182**, 103 (2000).
[21] B. E. Lehmann, H. Oeschger, H. H. Loosli, G. S. Hurst, S. L. Allman, C. H. Chen, S. D. Kramer, M. G. Payne, R. C. Phillips, R. D. Willis, and N. Thonnard, J. Geophys. Res. **90**, 11547 (1985).
[22] B. E. Lehmann, H. H. Loosli, D. Rauber, N. Thonnard, and R. D. Willis, Appl. Geochem. **6**, 419 (1991).
[23] C. Y. Chen, Y. M. Li, K. Bailey, T. P. O'Connor, L. Young, and Z. T. Lu, Science **286**, 1139 (1999).
[24] W. Jiang, K. Bailey, Z. T. Lu, P. Mueller, T. P. O'Connor, C. F. Cheng, S. M. Hu, R. Purtschert, N. Sturchio, Y. R. Sun, W. Williams, and G. M. Yang, Geochim. Cosmochim. Acta **91**, 1 (2012).
[25] G. M. Yang, C. F. Cheng, W. Jiang, Z. T. Lu, R. Purtschert, Y. R. Sun, L. Y. Tu, and S. M. Hu, Sci. Rep. **3**, 1 (2013).
[26] C. F. Cheng, W. Jiang, G. M. Yang, Y. R. Sun, H. Pan, Y. Gao, A. W. Liu, and S. M. Hu, Rev. Sci. Instrum. **81**, 123106 (2010).
[27] C. F. Cheng, G. M. Yang, W. Jiang, Y. R. Sun, L. Y. Tu, and S. M. Hu, Opt. Lett. **38**, 31 (2013).
[28] J. Smethie, M. William, and G. Mathieu, Marine Chem. **18**, 17 (1986).
[29] T. Ohta, Y. Mahara, N. Momoshima, F. Inoue, J. Shimada, R. Ikawa, and M. Taniguchi, J. Hydro. **376**, 152 (2009).
[30] L. Y. Tu, G. M. Yang, C. F. Cheng, G. L. Liu, X. Y. Zhang, and S. M. Hu, Anal. Chem. **86**, 4002 (2014).
[31] C. Schlosser and F. Klingberg, *Symposium on International Safeguards: Linking Strategy, Implementation and People*, Vienna, Austria, October 20−24 (2014).
[32] P. Collon, W. Kutschera, and Z. T. Lu, Annu. Rev. Nucl. Partic. Sci. **54**, 39 (2004).
[33] C. von Rohden, A. Kreuzer, Z. Chen, R. Kipfer, and W. Aeschbach-Hertig, Wat. Resour. Res. **46**, W05511 (2010).
[34] C. Buizert, D. Baggenstos, W. Jiang, R. Purtschert, V. V. Petrenko, Z. T. Lu, P. Müller, T. Kuhl, J. Lee, J. P. Severinghaus, and E. J. Brook, Proc. Nation. Acad. Sci. 1320329111 (2014).
[35] W. Jiang, W. Williams, K. Bailey, A. M. Davis, S. M. Hu, Z. T. Lu, T. P. O'Connor, R. Purtschert, N. C. Sturchio, Y. R. Sun, and P. Mueller, Phys. Rev. Lett. **106**, 103001 (2011).
[36] F. Ritterbusch, S. Ebser, J. Welte, T. Reichel, A. Kersting, R. Purtschert, W. Aeschbach- Hertig, and M. K. Oberthaler, Geophys. Res. Lett. **41**, 6758 (2014).
[37] W. S. Broecker and T. H. Peng, Nuc. Instrum. Meth. B **172**, 473 (2000).

DOI:10.1063/1674-0068/28/cjcp1505108